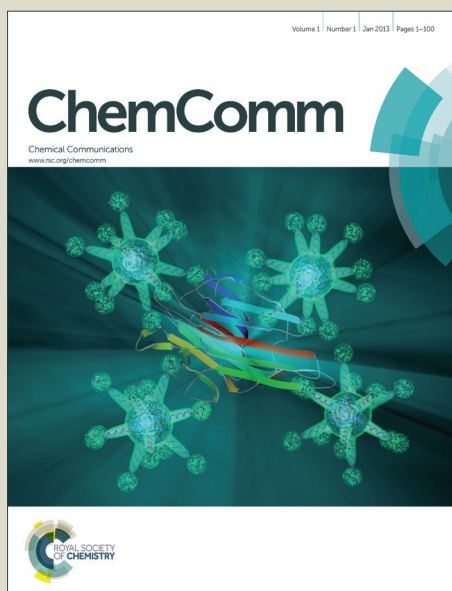


# ChemComm

Accepted Manuscript



This article can be cited before page numbers have been issued, to do this please use: H. XU, F. Han, X. Zhang, J. Zhang, Y. Wei, X. Zhang and W. Huang, *Chem. Commun.*, 2016, DOI: 10.1039/C6CC01414C.



This is an *Accepted Manuscript*, which has been through the Royal Society of Chemistry peer review process and has been accepted for publication.

*Accepted Manuscripts* are published online shortly after acceptance, before technical editing, formatting and proof reading. Using this free service, authors can make their results available to the community, in citable form, before we publish the edited article. We will replace this *Accepted Manuscript* with the edited and formatted *Advance Article* as soon as it is available.

You can find more information about *Accepted Manuscripts* in the [Information for Authors](#).

Please note that technical editing may introduce minor changes to the text and/or graphics, which may alter content. The journal's standard [Terms & Conditions](#) and the [Ethical guidelines](#) still apply. In no event shall the Royal Society of Chemistry be held responsible for any errors or omissions in this *Accepted Manuscript* or any consequences arising from the use of any information it contains.

Cite this: DOI: 10.1039/c0xx00000x

www.rsc.org/xxxxxx

ARTICLE TYPE

## 3D-Encapsulated Iridium-Complexed Nanophosphors for Highly Efficient Host-Free Organic Light-Emitting Diodes

Fuquan Han,<sup>a</sup> Xiaolin Zhang,<sup>b</sup> Jing Zhang,<sup>a</sup> Ying Wei,<sup>ac</sup> Xinwen Zhang,<sup>\*b</sup> Wei Huang<sup>bc</sup> and Hui Xu<sup>\*ac</sup>

Received (in XXX, XXX) Xth XXXXXXXXXX 200X, Accepted Xth XXXXXXXXXX 200X

DOI: 10.1039/b000000x

Iridium-complexed nanosize phosphors 3d-encapsulated with nine 3,6-di-*tert*-butyl-*N*-propyl-carbazole groups were constructed as host-dopant integrated systems, realizing the high photoluminescence quantum yield beyond 70% from neat evaporated films and electroluminescence external quantum efficiency up to ~8.5% and near-zero roll-offs at 1000 cd m<sup>-2</sup> from its dual-layer host-free light-emitting diodes.

The nano-pixel technology emerges in recent years for ultrahigh resolution displays with millions of dots per inch (DPI).<sup>1</sup> In comparison to pixel nanolithography, electroluminescent (EL) nano-size emitters are promising in device simplification since each emitter can be used as a pixel dot.<sup>2</sup> Quantum dots (QD) are the typical nanosize fluorophors for full-color light-emitting diodes (LED) with high EL efficiencies.<sup>3</sup> Since the dependence of emission color on QDs size, pixel size of various color QD-based displays should be different. Contrarily, the emissions of organic luminophors correspond to the bandgaps between their excited and ground states, which are dependent on conjugation and intramolecular electronic interplays rather than molecular size.<sup>4</sup> Therefore, organic EL materials can render the unique pixel sizes for their molecule-level super-resolution devices.

Polymers, dendrimers and oligomers are three main kinds of nano-scaled organic materials. Phosphorescent units should be involved in these materials to harvest all electrogenerated excitons. In this case, their superiority in host-dopant integration can be utilized for realizing single-molecular emissive layers (EML) with effective quenching suppression. In contrast to polydisperse polymeric phosphors, dendrimeric and oligomeric systems are dominant in uniformity, controllability and repeatability, making them more promising as single-molecular pixels. Up to now, there are many reports about high-performance solution-processed undoped phosphorescent organic LEDs (PHOLED) based on polymers,<sup>5</sup> dendrimers<sup>6</sup> and oligomers<sup>7</sup>, revealing the external quantum efficiency (EQE) around 4-10% with remarkable efficiency roll-offs. Our group reported a simple but effective strategy of carrier-transporting group and aliphatic chain (CTAC) mixed modification to develop host-dopant integrated multi-functional complexes,<sup>8</sup> in which Ir(III) complexes realized the maximum EQE of nearly 6%, but accompanied with EQE roll-off of 24% at 1000 cd m<sup>-2</sup>.<sup>8b</sup>

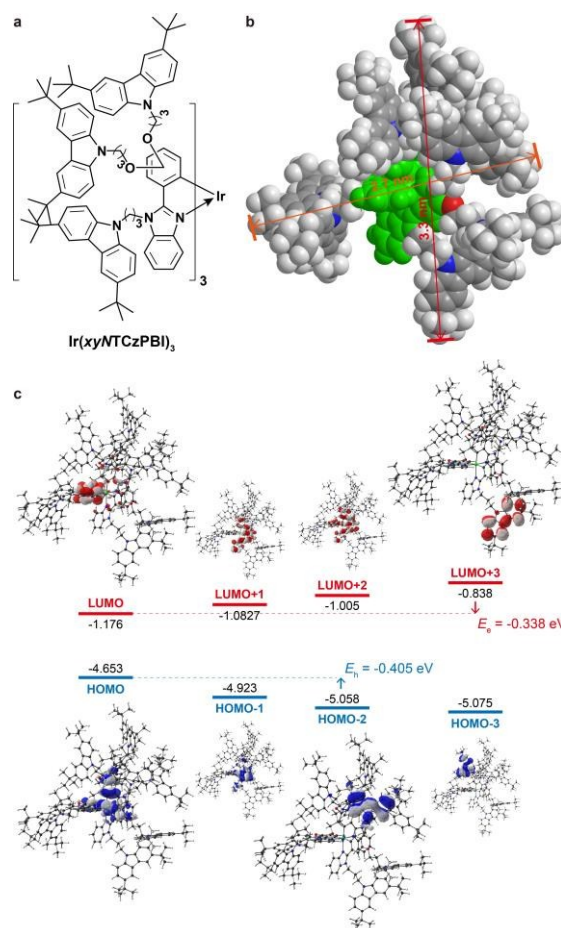


**Fig. 1** a. Chemical structure of Ir(xyNTCzPBI)<sub>3</sub>; b. Optimized ground-state molecular configuration and size of Ir(34NTCzPBI)<sub>3</sub>; c. Contours and energy levels of the first four occupied and unoccupied molecular orbitals for Ir(34NTCzPBI)<sub>3</sub> simulated with DFT method.

In this contribution, three Iridium-complexed nanosize phosphors collectively named Ir(xyNTCzPBI)<sub>3</sub> were constructed with analogous core-shell structures on the basis of CTAC strategy, whose Ir(PBI)<sub>3</sub> cores (PBI = phenylbenzimidazole) are encapsulated with 3,6-di-*tert*-butyl-*N*-propyl-carbazole (tbCz) groups (Fig. 1a and Scheme S1). Three tbCz groups were introduced in each PBI of the complex core through its *N*-H of imidazole and two ether bridges on phenyl to afford three-dimensional encapsulation of Ir(PBI)<sub>3</sub> core with as many as nine

**tbCzp** groups at various directions.  $x$  and  $y$  in the collective name of  $\text{Ir}(xy\text{NTCzPBI})_3$  refer to the substitution positions of ether bridges, viz. 2,3, 2,4 and 3,4, respectively. The host feature of carbazole group in **tbCzp** with high triplet energy and good carrier transporting ability can support the efficient energy and charge transfer to the emissive cores.<sup>9</sup> The most uniformly dispersed **tbCzp** groups endowed  $\text{Ir}(34\text{NTCzPBI})_3$  with the state-of-the-art performance of its solution-processed nondoped bilayer devices, especially EQE beyond 8% and negligible roll-off at  $1000 \text{ cd m}^{-2}$ , which successfully manifests the great potential of CTAC-type phosphors as single-molecular nano-emitters for the super-resolution displays.

According to density functional theory (DFT) simulation on  $\text{Ir}(xy\text{NTCzPBI})_3$ , the spatial extension directions of **tbCzp** groups at 2 and  $N$ -positions are overlapping, which are separate to **tbCzp** groups at 3 and 4-positions. In this case, the configuration of  $\text{Ir}(34\text{NTCzPBI})_3$  is the closest to sphere, accompanied by the biggest molecular volume ( $\phi \approx 3 \text{ nm}$ ) (Fig. 1b), which is consistent with its atom force microscopy (AFM) pattern (Fig. S1). The nine **tbCzp** groups in  $\text{Ir}(34\text{NTCzPBI})_3$  are almost uniformly distributed around  $\text{Ir}(\text{PBI})_3$  core to form an effective 3d shell, protecting it from intermolecular interaction-induced quenching. The highest occupied and lowest unoccupied molecular orbitals (HOMO and LUMO), as well as the HOMO-1, the LUMO+1 and the LUMO+2, of  $\text{Ir}(34\text{NTCzPBI})_3$  are mainly contributed by its  $\text{Ir}(\text{PBI})_3$  core, in which the HOMO is dispersed on phenyl of PBI and  $\text{Ir}^{3+}$  ion; while, the LUMO is concentrated on benzimidazole of PBI. In this sense, the peripheral **tbCzp** groups hardly influence the emission of the complex (Fig. 1c). However, it is noteworthy that the HOMO-2 and the LUMO+3 of  $\text{Ir}(34\text{NTCzPBI})_3$  are localized on its carbazole moieties, making **tbCzp** groups involved in carrier injection and transport process. The remarkable energy gaps between the first frontier molecular orbitals (FMO) on  $\text{Ir}(\text{PBI})_3$  core and **tbCzp** groups can generate the efficient charge traps on  $\text{Ir}(\text{PBI})_3$  core with large depths of 0.41 and 0.39 eV for hole and electron, respectively, which can enhance the direct recombination and confinement of excitons on emissive center and reduce energy loss during irradiative exciton-migration processes.

In dilute solution, the electronic absorption bands of  $\text{Ir}(xy\text{NTCzPBI})_3$  from the  $n \rightarrow \pi^*$  and  $\pi \rightarrow \pi^*$  transitions of the ligands in the range of 200–350 nm are identical with the same and profiles (Fig. 2a). However,  $\text{Ir}(34\text{NTCzPBI})_3$  reveals the strongest absorption tail characteristic of mixed metal-ligand charge transfer (<sup>3</sup>MLCT) and ligand-ligand charge transfer (<sup>3</sup>LLCT), which should be owing to its most planar PBI moieties supported by 3,4-substitution with the smallest steric hindrance. As shown by the emission fine structures in low-temperature emissions (inset of Fig. 2a), the different resonance effects between ether bridges at 2 (*ortho*-), 3 (*meso*-) and 4 (*para*-) positions and imidazole render the various bandgaps for  $\text{Ir}(xy\text{NTCzPBI})_3$ , corresponding to yellow, bluish green and green emissions from  $\text{Ir}(23\text{NTCzPBI})_3$ ,  $\text{Ir}(24\text{NTCzPBI})_3$  and  $\text{Ir}(34\text{NTCzPBI})_3$  with peaks at 563, 505 and 523 nm, respectively, accompanied by photoluminescence quantum yields (PLQY) of 52%, 75% and 73% and lifetimes ( $\tau$ ) of 7.8, 6.5 and 6.5  $\mu\text{s}$  (Fig. S2 and Table S1). The pure  $\text{Ir}^{3+}$  complex-originated emissions under 350 nm excitation verify the efficient energy

transfer from peripheral **tbCzp** groups to emissive cores. The spin-coated thin films of  $\text{Ir}(xy\text{NTCzPBI})_3$  show the preserved absorption fine structures and slight emission shifts within 10 nm (Fig. S4a). Nevertheless, in contrast to the almost unchanged  $\tau$  of  $\text{Ir}(24\text{NTCzPBI})_3$  and  $\text{Ir}(34\text{NTCzPBI})_3$  as  $\sim 6.2 \mu\text{s}$ ,  $\tau$  of  $\text{Ir}(23\text{NTCzPBI})_3$  is remarkably decreased to 6.1  $\mu\text{s}$ , indicating the worsened quenching due to the interactions between  $\text{Ir}(\text{PBI})_3$  cores in adjacent molecules, which is consistent with the deficient protection effect of its most overlapped **tbCzp** groups (Fig. S4b). It is rational that owing to the most uniform dispersion of **tbCzp** groups,  $\text{Ir}(34\text{NTCzPBI})_3$  film further reveals the highest PLQY of 72%, equivalent to that in solution and remarkably higher than 35% and 64% of  $\text{Ir}(23\text{NTCzPBI})_3$  and  $\text{Ir}(24\text{NTCzPBI})_3$ .

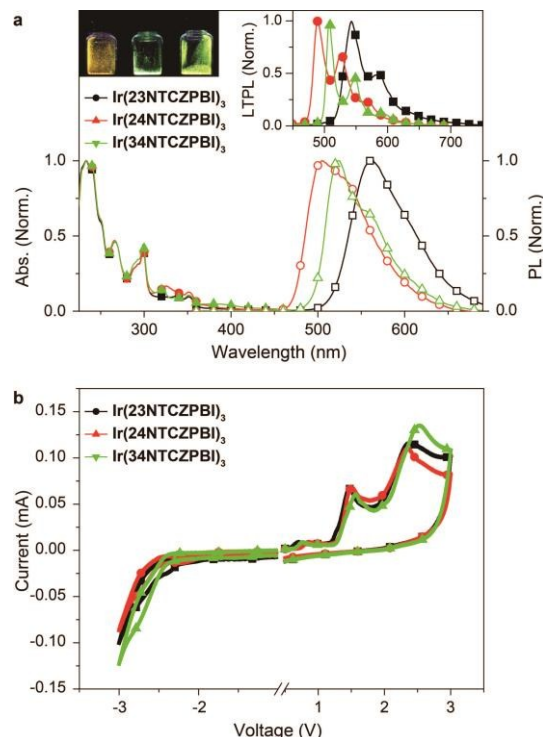


**Fig. 2 a.** UV/vis absorption (abs.) and photoluminescence (PL) spectra of  $\text{Ir}(xy\text{NTCzPBI})_3$  in degassed  $\text{CH}_2\text{Cl}_2$  ( $10^{-6} \text{ mol L}^{-1}$ ) at room temperature. Insets: emissive photos under 365 nm excitation and low-temperature PL (LTPL) spectra measured at 77 K; **b.** Cyclic voltammograms of  $\text{Ir}(xy\text{NTCzPBI})_3$  measured at room temperature under  $\text{N}_2$ .

The electrochemical properties of  $\text{Ir}(xy\text{NTCzPBI})_3$  exhibit the direct evidences of the emission variation (Fig. 2b). All of the complexes have the similar anodic and cathodic peaks attributed to the oxidations of  $\text{Ir}^{3+}$ , phenyl of PBI and **tbCzp** and the reduction of imidazole, respectively. No couple-originated peaks from **tbCzp** are observed, in spite of its irreversible oxidation waves. However, the evaluated HOMO and LUMO levels of  $\text{Ir}(23\text{NTCzPBI})_3$ ,  $\text{Ir}(24\text{NTCzPBI})_3$  and  $\text{Ir}(34\text{NTCzPBI})_3$  are -5.35, -5.49 and -5.42 eV and -2.69, -2.34 and -2.41 eV, respectively, which is ascribed to the different resonance effects of their ether bridges as shown by optical analysis.

The efficient shell-to-core energy and charge migration encouraged us to fabricate host-free devices of  $\text{Ir}(xy\text{NTCzPBI})_3$  through spin coating with a conventional bilayer configuration of ITO|PEDOT:PSS (50nm)| $\text{Ir}(xy\text{NTCzPBI})_3$  (40nm)|TPBi (30nm)|LiF (1nm)|Al (Scheme S2). The EL spectra identical to PL

manifested the complete exciton confinement on the emissive cores of these phosphors (inset of Fig. 3a). **Ir(34NTCzPBI)<sub>3</sub>** endowed its devices with the significantly low driving voltages of 3.5 V for onset, <5.0 V and <6.0 V at 100 and 1000 cd m<sup>-2</sup>, which were several voltages lower than those of other devices (Fig. 3a and Table S2). **Ir(34NTCzPBI)<sub>3</sub>** further realized the highest efficiencies with the maxima of 27.7 cd A<sup>-1</sup> for current efficiency (CE), 15.4 lm W<sup>-1</sup> for power efficiency (PE) and 8.3% for EQE, accompanied with the negligible efficiency roll-offs as low as 0.4% at 1000 cd m<sup>-2</sup> for EQE (Fig. 3b and Table S2). In contrast, the lowest device efficiencies of **Ir(23NTCzPBI)<sub>3</sub>** were in accord with its worst optical properties, due to its distorted configuration for non-radiative transition and deficient encapsulation for exciton quenching. The excellent comprehensive EL performance of **Ir(34NTCzPBI)<sub>3</sub>** makes it among the best solution-processable phosphors for host-free devices. It is noteworthy that when using TCTA as host, the EL performance of **Ir(34NTCzPBI)<sub>3</sub>**-doped devices was instead decreased, contrary to the situations of other two phosphors (Fig. S5). In this case, in comparison to its analogues, the main reason for the best EL performance of **Ir(34NTCzPBI)<sub>3</sub>** should be attributed to its most uniformly dispersed **tbCzp** groups, whose efficacy in energy and carrier transfer and emissive center isolation can be comparable and even superior to host matrix.

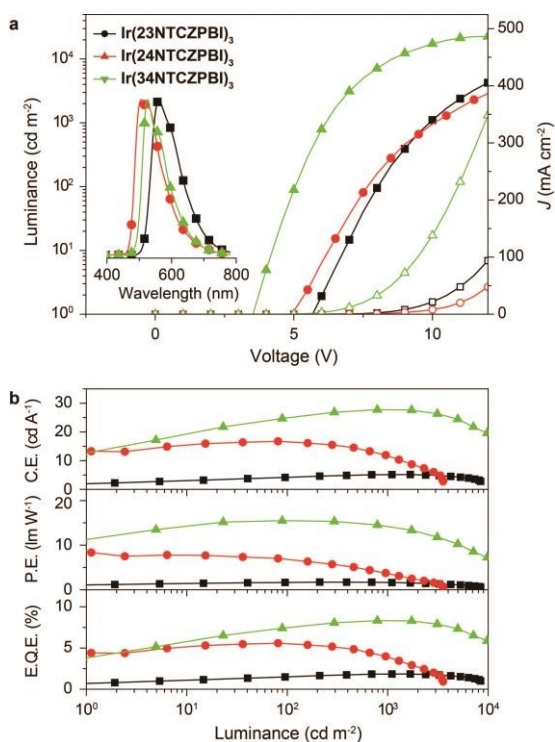


**Fig. 3 a.** EL spectra (inset) and luminance-current density ( $J$ )-voltage curves of **Ir(xyNTCzPBI)<sub>3</sub>**-based bilayer spin-coated OLEDs; **b.** Efficiency vs. luminance relationships of the devices.

In summary, a series of nanosize phosphors **Ir(xyNTCzPBI)<sub>3</sub>** featured host-dopant integrated core-shell structure were constructed on the basis of CTAC strategy. With the most uniformly dispersed **tbCzp** groups, **Ir(34NTCzPBI)<sub>3</sub>** realizes the best optoelectronic properties, indicating the significance of the peripheral-group distribution. The impressive EL performance of its spin-coated nondoped devices makes it competent as single-

molecular EMLs for super-resolution devices.

F.H. and X.Z. contributed equally to this work. This project was financially supported by NSFC (51373050), Education Bureau of Heilongjiang Province (2014CJHB005) and the Fok Ying-Tong Education Foundation for Young Teachers in the Higher Education Institutions of China (141012).

## Notes and references

- <sup>a</sup> Key Laboratory of Functional Inorganic Material Chemistry, School of Chemistry and Materials, Heilongjiang University, Ministry of Education, Harbin 150080, China. E-mail: hxu@hlju.edu.cn.
- <sup>b</sup> Key Laboratory for Organic Electronics and Information Displays (KLOEID), Institute of Advanced Materials (IAM), Nanjing University of Posts and Telecommunications, 9 Wenyuan Road, Nanjing 210023, China. E-mail: iamxwzhang@njupt.edu.cn.
- <sup>c</sup> Key Laboratory of Flexible Electronics (KLOFE) & Institute of Advanced Materials (IAM), Jiangsu National Synergetic Innovation Center for Advanced Materials (SICAM), Nanjing Tech University (NanjingTech), 30 South Puzhu Road, Nanjing 211816, China.
- † Electronic Supplementary Information (ESI) available: Experimental details, AFM images, thermal properties, optical properties and EL performance data of the doped devices. See DOI: 10.1039/b000000x/
- (a) R. J. Walters, G. I. Bourianoff and H. A. Atwater, *Nat Mater*, 2005, 4, 143; (b) Y. Shirasaki, G. J. Supran, M. G. Bawendi and V. Bulovic, *Nat Photon*, 2013, 7, 13.
  - (a) M. Tan, P. Munusamy, V. Mahalingam and F. C. J. M. van Veggel, *J. Am. Chem. Soc.*, 2007, 129, 14122; (b) F. Wang, Y.-h. Chen, C.-y. Liu and D.-g. Ma, *Chem. Commun.*, 2011, 47, 3502.
  - (a) X. Dai, Z. Zhang, Y. Jin, Y. Niu, H. Cao, X. Liang, L. Chen, J. Wang and X. Peng, *Nature*, 2014, 515, 96; (b) L. Qian, Y. Zheng, J. Xue and P. H. Holloway, *Nat Photon*, 2011, 5, 543; (c) K.-S. Cho, E. K. Lee, W.-J. Joo, E. Jang, T.-H. Kim, S. J. Lee, S.-J. Kwon, J. Y. Han, B.-K. Kim, B. L. Choi and J. M. Kim, *Nat Photon*, 2009, 3, 341; (d) D. I. Son, B. W. Kwon, D. H. Park, W.-S. Seo, Y. Yi, B. Angadi, C.-L. Lee and W. K. Choi, *Nat Nano*, 2012, 7, 465.
  - H. Xu, R. Chen, Q. Sun, W. Lai, Q. Su, W. Huang and X. Liu, *Chem. Soc. Rev.*, 2014, 43, 3259.
  - (a) H. Zhen, C. Jiang, W. Yang, J. Jiang, F. Huang and Y. Cao, *Chem. Eur. J.*, 2005, 11, 5007; (b) S.-J. Liu, Q. Zhao, R.-F. Chen, Y. Deng, Q.-L. Fan, F.-Y. Li, L.-H. Wang, C.-H. Huang and W. Huang, *Chem. Eur. J.*, 2006, 12, 4351; (c) H. Zhen, J. Luo, W. Yang, Q. Chen, L. Ying, Z. Jianhua, H. Wu and Y. Cao, *J. Mater. Chem.*, 2007, 17, 2824; (d) W.-S. Huang, Y.-H. Wu, H.-C. Lin and J. T. Lin, *Polym. Chem.*, 2010, 1, 494; (e) S. Shao, Z. Ma, J. Ding, L. Wang, X. Jing and F. Wang, *Adv. Mater.*, 2012, 24, 2009; (f) L. Ying, C.-L. Ho, H. Wu, Y. Cao and W.-Y. Wong, *Adv. Mater.*, 2014, 26, 2459; (g) X. Yang, G. Zhou and W.-Y. Wong, *J. Mater. Chem. C*, 2014, 2, 1760.
  - (a) P. L. Burn, S. C. Lo and I. D. W. Samuel, *Adv. Mater.*, 2007, 19, 1675; (b) J. Ding, J. Gao, Y. Cheng, Z. Xie, L. Wang, D. Ma, X. Jing and F. Wang, *Adv. Funct. Mater.*, 2006, 16, 575; (c) G. Zhou, W.-Y. Wong, B. Yao, Z. Xie and L. Wang, *Angew. Chem. Int. Ed.*, 2007, 119, 1167; (d) D. Xia, B. Wang, B. Chen, S. Wang, B. Zhang, J. Ding, L. Wang, X. Jing and F. Wang, *Angew. Chem. Int. Ed.*, 2014, 53, 1048; (e) X. Xu, X. Yang, J. Zhao, G. Zhou and W.-Y. Wong, *Asian J. Org. Chem.*, 2015, 4, 394.
  - (a) C. Liu, Y. Li, Y. Li, C. Yang, H. Wu, J. Qin and Y. Cao, *Chem. Mater.*, 2013, 25, 3320; (b) B. Chen, J. Ding, L. Wang, X. Jing and F. Wang, *Chem. Commun.*, 2012, 48, 8970.
  - (a) H. Xu, Z.-F. Xu, Z.-Y. Yue, P.-F. Yan, B. Wang, L.-W. Jia, G.-M. Li, W.-B. Sun and J.-W. Zhang, *J. Phys. Chem. C*, 2008, 112, 15517; (b) H. Xu, D.-H. Yu, L.-L. Liu, P.-F. Yan, L.-W. Jia, G.-M. Li and Z.-Y. Yue, *J. Phys. Chem. B*, 2010, 114, 141; (c) J.-X. Cai, T.-L. Ye, X.-F. Fan, C.-M. Han, H. Xu, L.-L. Wang, D.-G. Ma, Y. Lin and P.-F. Yan, *J. Mater. Chem.*, 2011, 21, 15405.
  - (a) W.-Y. Wong and C.-L. Ho, *J. Mater. Chem.*, 2009, 19, 4457; (b) W.-Y. Wong, *Coord. Chem. Rev.*, 2005, 249, 971; (c) W.-Y. Wong and C.-L. Ho, *Coord. Chem. Rev.*, 2009, 253, 1709.